

Examination of Mixed-Phase Precipitation Forecasts from the High-Resolution Rapid Refresh Model Using Surface Observations and Sounding Data

KYOKO IKEDA, MATTHIAS STEINER, AND GREGORY THOMPSON

National Center for Atmospheric Research,^a Boulder, Colorado

(Manuscript received 22 September 2016, in final form 6 January 2017)

ABSTRACT

Accurate prediction of mixed-phase precipitation remains challenging for numerical weather prediction models even at high resolution and with a sophisticated explicit microphysics scheme and diagnostic algorithm to designate the surface precipitation type. Since mixed-phase winter weather precipitation can damage infrastructure and produce significant disruptions to air and road travel, incorrect surface precipitation phase forecasts can have major consequences for local and statewide decision-makers as well as the general public. Building upon earlier work, this study examines the High-Resolution Rapid Refresh (HRRR) model's ability to forecast the surface precipitation phase, with a particular focus on model-predicted vertical temperature profiles associated with mixed-phase precipitation, using upper-air sounding observations as well as the Automated Surface Observing Systems (ASOS) and Meteorological Phenomena Identification Near the Ground (mPING) observations. The analyses concentrate on regions of mixed-phase precipitation from two winter season events. The results show that when both the observational and model data indicated mixed-phase precipitation at the surface, the model represents the observed temperature profile well. Overall, cases where the model predicted rain but the observations indicated mixed-phase precipitation generally show a model surface temperature bias of $<2^{\circ}\text{C}$ and a vertical temperature profile similar to the sounding observations. However, the surface temperature bias was $\sim 4^{\circ}\text{C}$ in weather systems involving cold-air damming in the eastern United States, resulting in an incorrect surface precipitation phase or the duration (areal coverage) of freezing rain being much shorter (smaller) than the observation. Cases with predicted snow in regions of observed mixed-phase precipitation present subtle difference in the elevated layer with temperatures near 0°C and the near-surface layer.

1. Introduction

Subtle changes in the vertical structure of cold-season precipitating weather systems determine the form of precipitation reaching the ground. Whether precipitation at the surface is liquid (rain), solid (snow, graupel, ice pellets), or mixed phase (herein, mixed phase is either a mixture of both liquid and solid precipitation particles, solely freezing drizzle, or freezing rain since it forms ice upon contact with surface objects) significantly influences the decision-making for air traffic operations and road weather management. It impacts city operations (e.g., school and business closures), and it may cause infrastructure damage (e.g., Changnon 2003; Goodwin 2003;

Call 2005, 2010; Grout et al. 2012). Thus, it is essential that weather forecast models accurately predict precipitation type or phase reaching the surface both in space and time.

Ikeda et al. (2013) evaluated the ability of the operational High-Resolution Rapid Refresh (HRRR) forecast model to properly determine the surface precipitation phase as rain, snow, or mixed phase from the 2010/11 winter season. The study found that the HRRR model reliably predicted the areal extent of snow and rain compared with Automated Surface Observing Systems (ASOS; National Weather Service 1998) reports. Qualitatively, the agreement was also good in regions of rain–snow transition and for freezing precipitation when examining the spatial coverage and temporal consistency versus observations. Quantitatively speaking, however, the model performance was less skillful in regions of mixed-phase precipitation compared with the rain and snow regions, pointing out the need for diagnosing potential model shortcomings in these areas.

^a The National Center for Atmospheric Research is sponsored by the National Science Foundation.

Corresponding author e-mail: Kyoko Ikeda, kyoko@ucar.edu

[Ikeda et al. \(2013\)](#) showed that a model bias in surface temperature was partly responsible for the reduced prediction skill in the mixed-phase region. In particular, they found a $\sim 2^{\circ}\text{C}$ warm bias when the model incorrectly predicted rain in the area of observed mixed-phase precipitation with the observed temperature near freezing. In addition, a cold bias of $\sim 2^{\circ}\text{--}4^{\circ}\text{C}$ was found when the model forecasted snow but mixed-phase precipitation was observed and the temperature was close to 0°C . Another possible reason for forecast errors suggested by [Ikeda et al. \(2013\)](#), but not yet investigated, included inaccurate prediction of the thermodynamic and microphysical vertical structure by the HRRR model. In the present study, we expand upon the work of [Ikeda et al. \(2013\)](#) to take a closer look at the HRRR model's vertical profiles near mixed-phase precipitation areas, aiming to understand some of the model features in these regions and assessing whether the model adequately captured the observed vertical thermodynamic profiles. Routine upper-air sounding observations were used to compare with the HRRR model profiles. The number of cases that could be evaluated is limited by the availability of sounding data at the right location and time. Nonetheless, this study provides further insight into incorrect forecasts of precipitation phase that may guide model enhancement and development.

Making correct forecasts of mixed-phase precipitation, freezing rain, and ice pellets is challenging. The thermodynamic conditions in the rain–snow transition regions of winter storms are continuously changing (from local to mesoscale), yielding various types of precipitation ([Stewart 1992](#)). The latent heat effect from the melting and freezing of precipitating particles can further complicate the temperature and humidity profiles near the rain–snow boundary (e.g., [Stewart 1985](#); [Lackmann et al. 2002](#)). Additionally, small differences in the thermodynamic structure aloft can impact the precipitation form and type falling to the ground (e.g., [Rauber et al. 2001](#); [Thériault et al. 2010](#); [Sims and Liu 2015](#); [Reeves et al. 2016](#); [Sankaré and Thériault 2016](#)). In particular, the vertical thermodynamic structures of ice pellets and freezing rain are so similar that any forecast uncertainty, which may affect the thickness of an elevated melting layer and a near-surface refreezing layer, can result in an incorrect prediction of the surface precipitation type ([Reeves et al. 2014](#); [Reeves et al. 2016](#)). Additionally, snowflake types and lapse rate aloft can yield differences in the precipitation phase and/or type reaching the surface as a result of changes in the time required to melt snow crystals falling through the melting layer and refreeze partially melted precipitating particles ([Sankaré and Thériault 2016](#)). The precipitation rate below the melting layer directly impacts the surface temperature

through cooling effects; yet, the precipitation rate is influenced by the type of snowflakes found aloft that continuously evolve in their shape, density, and degree of riming, and interact with other particles while falling through atmospheric layers of various temperatures and moisture levels (e.g., [Stewart et al. 2015](#); [Sankaré and Thériault 2016](#); [Reeves et al. 2016](#)). These challenges point to the fact that the ability of a forecast model to represent correctly the thermodynamic conditions aloft and near the surface is critical for making accurate precipitation phase forecasts at the surface.

This paper is organized as follows. [Section 2](#) provides a description of the forecast model and the observational datasets. The cases examined in this study are briefly discussed in [section 3](#). Results are presented in [section 4](#), followed by a summary and concluding remarks in [section 5](#).

2. Forecast model and observational datasets

a. High-Resolution Rapid Refresh

The study utilizes forecast data generated by the hourly updating HRRR model that is run in real time at the National Oceanic and Atmospheric Administration/Earth System Research Laboratory (NOAA/ESRL) (e.g., [Benjamin et al. 2016a](#)). The HRRR is a cloud-permitting numerical weather prediction model that builds on the Advanced Research core of the Weather Research and Forecasting (WRF) Model ([Skamarock et al. 2008](#)) with 3-km horizontal grid spacing and 50 vertical levels whose domain covers the contiguous United States. The HRRR model domain is nested within the larger 13-km Rapid Refresh (RAP; [Benjamin et al. 2016a](#)) parent model domain. The microphysical scheme used in the HRRR prior to 2015 was the [Thompson et al. \(2008\)](#) microphysics. In 2015, RAP version 3 and HRRR version 2 became operational at NOAA/ESRL with the aerosol-aware [Thompson and Eidhammer \(2014\)](#) scheme, as discussed in [Benjamin et al. \(2016b\)](#).

For each hour, the HRRR model assigns the surface precipitation *type* as one or more of rain, snow, ice pellets, or freezing rain based on a postprocessing routine in the operational HRRR forecasting system ([Ikeda et al. 2013](#); [Benjamin et al. 2016b](#)). Prior to 2015, the postprocessing routine examined vertical profiles of the rain, snow, and graupel mixing ratios fields from the explicit microphysical scheme and temperature to classify surface precipitation type as some combination of rain, snow, ice pellets, and/or freezing rain based on the diagnostic logic explained in Table 1 of [Ikeda et al. \(2013\)](#). The diagnostic routine for predicting precipitation type in the HRRR forecasting system has evolved based on the analyses presented by [Ikeda et al. \(2013\)](#)

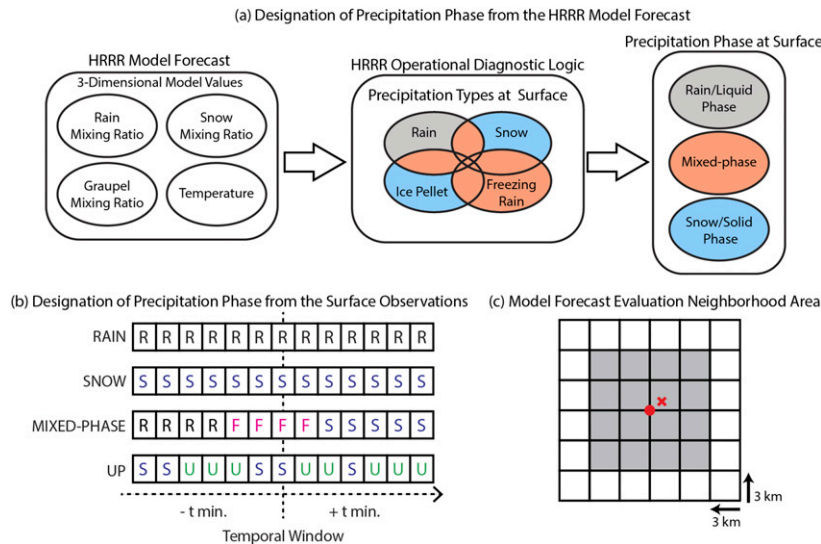


FIG. 1. (a) A flowchart illustrating how snow, rain, and mixed-phase precipitation is assigned to each model grid cell based on HRRR model forecasts of categorical surface precipitation types. The operational diagnostic logic used prior to the updates in Benjamin et al. (2016b) is described in Ikeda et al. (2013). (b) A schematic showing how the observed precipitation phase is determined from 1-min ASOS data and mPING data during a $\pm t$ -min temporal window, centered at a model valid time. (c) A spatial neighborhood box of a given width (gray-shaded area) centered at the closest grid point (red dot) from a surface site (red cross). The model predictions at every grid point inside the neighborhood box are used for evaluation.

and recent enhancement efforts at ESRL. An upgraded diagnostic precipitation type (p-type) scheme was implemented into the operational system in late 2015. The upgraded version of the diagnosis scheme is described in Benjamin et al. (2016b), and its performance has been evaluated by Elmore et al. (2015) and Burg et al. (2017).

The cases examined in this study occurred prior to the implementation of the upgraded p-type diagnostic scheme; therefore the model dataset of precipitation types were from the logic described in Table 1 of Ikeda et al. (2013). Burg et al. (2017) examined a handful of winter storms comparing the upgraded version to the previous version of the diagnostic scheme. They have shown that while there was some improvement to the ice pellet and snow forecasts, performance was nearly the same for rain, whose skill was already high, and not much improvement was seen for freezing rain. Thus, the results presented herein are likely to remain valid for the newer precipitation-type algorithm.

Each precipitation type is represented in four separate dichotomous data fields in the operational HRRR model dataset (Fig. 1a). More than one type of precipitation is permitted at a given grid point. For the cases examined in this study, we took the four precipitation-type data types and derived three precipitation *phase* categories (snow, rain, and mixed phase) to compare with the surface observations, as in Ikeda et al. (2013).

The operational HRRR model simulates out to 15 h with a data output increment of 1 h. Here, we focus on validating hourly forecasts of the precipitation phase with a lead time of 8 h against surface observations (discussed in the following subsection). We choose to evaluate only the 8-h forecasts, because Ikeda et al. (2013) have found the forecast performance of the precipitation phase to change very little after 4–5-h lead times for cold-season weather systems that are typically forced by large-scale synoptic weather systems.

Comparison with routine upper-air soundings was based on the 8-h forecasts valid at 0000 and 1200 UTC.¹ The model profiles were based on their native terrain-following vertical coordinate system and taking the average of data values from the four grid cells nearest to a sounding site.

b. Observational dataset

One-minute ASOS data were used to assess the skill of the hourly HRRR model forecasts of the surface

¹ In practice, upper-air soundings are launched at ~ 1100 and ~ 2300 UTC for reporting the 1200 and 0000 UTC sounding observations. The results presented herein did not change when model data valid at 1100 and 2300 UTC were compared to the sounding observations.

precipitation phase. The occurrence of snow (solid-phase particles), rain (liquid-phase particles), unknown precipitation (UP), or no precipitation (NP) is recorded every minute at over 800 ASOS stations nationwide using an optical precipitation detection sensor, which determines particle type depending on its terminal velocity² (National Weather Service 1998; Wade 2003). UP is an indication of the occurrence of light precipitation, such as light snow and drizzle, but the intensity is too low to determine whether the precipitation is frozen or in liquid phase. Ice pellets are not identified by the automated precipitation identifying sensor but are recognized either as rain, snow, or UP depending on their terminal velocity. The occurrence of ice pellets can only be confirmed if a human observer augments the ASOS reports. Only a small percentage of sites are manned. To make data from sites with a human observer consistent with those from sites without a human observer, human-augmented data were not used to compute forecast skill scores; however, they were still examined when non-augmented ASOS reports seemed erroneous.³

The raw ASOS precipitation-type dataset was carefully quality controlled for spatial and temporal consistency first because the ASOS precipitation-type algorithm may falsely report blowing snow as freezing rain and has a tendency to identify ice pellets as rain or UP (National Weather Service 1998). The ASOS icing sensor (e.g., Ramsay 1997) data, where available, were checked for the indication of freezing drizzle/rain (i.e., a rapid decrease in the vibrating probe frequency). Then, at each ASOS site, the data were assigned as rain, snow, or mixed-phase precipitation following the classification scheme of Ikeda et al. (2013; Fig. 1b). Observations over a temporal window of ± 6 min centered on the hour were used and classified as mixed phase when a rain-to-snow or snow-to-rain transition, or freezing rain, occurred within that time frame. If only snow was reported, or snow and UP occurred during the time window but no rain, the more frequently reported of the two was chosen. The assignment of rain was based on a similar logic as for snow.

Another observational dataset used in this study is from the Meteorological Phenomena Identification Near the Ground (mPING) project (Elmore et al. 2014; Elmore et al. 2015). The mPING database is based

upon a volunteer-reporting system via a smart phone application or the Internet. The database provides useful information, especially in regions where ASOS stations are sparse and the precipitation phase/type is actively changing. The mPING database provides the coordinates, time of observation, and precipitation type as rain, snow, ice pellets, freezing rain, drizzle, graupel, or hail. More than one type is possible in a single report (e.g., rain and snow). Some reports specifically say “no precipitation” before or after a precipitation event. The precipitation phase was assigned for mPING reports in the following manner: if only snow (rain) was reported, then it was put in the solid (liquid) precipitation phase category. If there was snow and rain, snow and freezing rain, or ice pellets and rain (or freezing rain) within a single report, then the observation was put into the mixed-phase precipitation category. Reeves (2016) compared ASOS and mPING datasets and found that mPING’s precipitation-type reports tend to shift from rain and freezing rain toward ice pellets at temperatures near freezing, which makes physical sense; whereas nonaugmented ASOS sites are incapable of reporting ice pellets. Because of the uncertainties associated with the mPING data, we calculated forecast skill scores using ASOS and mPING data independently as well as combined and found similarly robust results. The quantitative discussions hereafter are based on numerical values from the ASOS data assessment, whereas the mPING data are included in qualitative considerations since they increase data density in various case studies.

Evaluation of the vertical structure of model-predicted thermodynamic features was performed with the routine radiosonde data collected by the National Weather Service at 0000 and 1200 UTC. The upper-air sounding sites are typically equipped with an ASOS system (e.g., Reeves et al. 2014, their Fig. 1) or there is a close-by ASOS site. The observed precipitation phase corresponding to each sounding site is based on the collocated or nearby ASOS site. The surface temperature and precipitation rate observations that are shown in this study also come from the ASOS dataset.

3. Case selection

In this study we examine cases from the 2013/14 and 2014/15 winter seasons that represent precipitation events where mixed-phase precipitation or a snow-to-rain transition (and vice versa) occurred at a sounding site close to the routine observation time. Also, we focus on precipitation systems east of the Rocky Mountains, as in Ikeda et al. (2013). Table 1 summarizes the event

² For a more detailed discussion of how ASOS determines the precipitation type, refer to Ikeda et al. (2013).

³ Because ice pellets and freezing rain are infrequently predicted and over much smaller regions than rain and snow, the forecast skill scores of the precipitation phase (Table 2, section 4a) change very little even when human-augmented ASOS reports are used to compute the skill scores.

TABLE 1. Day, time (UTC), and location of sounding comparisons. Observed and model surface precipitation phase are also indicated in the observation and model columns, respectively. A unique event identifier (the event column) is assigned to each case examined in this study and used throughout; the event identifier is based on a letter and number combination.

Event	Day and Time	Sounding Site	Site ID	Observation	Model
A1	1200 UTC 26 Nov 2013	Sterling, VA	IAD	Rain	Rain
A2		Greensboro, NC	GSO	Mix	Rain
A3	0000 UTC 27 Nov 2013	Sterling, VA	IAD	Rain	Rain
A4		Greensboro, NC	GSO	Rain	Rain
B1	1200 UTC 6 Dec 2013	Wilmington, OH	ILN	Mix	Mix
B2		Springfield, MO	SGF	Snow	Snow
B3		Little Rock, AR	LZK	Mix	Mix
B4		Fort Worth, TX	FWD	Mix	Mix
C1	1200 UTC 14 Dec 2013	Wilmington, OH	ILN	Mix	Mix
C2	0000 UTC 15 Dec 2013	Washington, DC	IAD	Rain	Rain
C3		Pittsburgh, PA	PIT	Rain	Rain
D1	1200 UTC 21 Dec 2013	Lincoln, IL	ILX	Mix	Mix
D2		Springfield, MO	SGF	Mix	Rain
D3		Norman, OK	OUN	Mix	Mix
D4	0000 UTC 22 Dec 2013	Lincoln, IL	ILX	Mix	Mix
D5		Springfield, MO	SGF	Rain	Rain
D6		Topeka, KS	TOP	Mix	Snow
D7		Detroit, MI	DTX	Mix	Mix
E1	0000 UTC 12 Jan 2015	Lincoln, IL	ILX	Mix	Mix
E2		Wilmington, OH	ILN	Rain	Mix
E3	1200 UTC 12 Jan 2015	Sterling, VA	IAD	Mix	Rain
E4		Roanoke, VA	RNK	Rain	Rain
F1	0000 UTC 24 Jan 2015	Sterling, VA	IAD	Mix	Rain
F2		Roanoke, VA	RNK	Mix	Rain
F3	1200 UTC 24 Jan 2015	Brookhaven, NY	OKX	Mix	Rain
G1	1200 UTC 26 Jan 2015	Sterling, VA	IAD	Mix	Rain
H1	0000 UTC 22 Feb 2015	Brookhaven, NY	OKX	Snow	Snow
H2		Sterling, VA	IAD	Mix	Snow
H3	1200 UTC 22 Feb 2015	Brookhaven, NY	OKX	Rain	Mix

designation, day and time, and sounding locations, as well as observed and predicted precipitation phase examined in this study, and Fig. 2 shows maps of 8-h precipitation phase forecasts valid at the time of the observed sounding. The sounding data availability at the right time and location limits the number of cases, and they are all from large synoptically-driven precipitation systems. The cases include precipitation systems that produced a well-defined mixed-phase precipitation area or prolonged freezing rain [6 December 2013 (event C), 21 December 2013 (event D), 22 December 2013 (event D), and 12 January 2015 (event E)], freezing rain caused by cold-air damming to the east of the Appalachian Mountains [26 November 2013 (event A) and 12 January 2015 (event E)], and a narrow snow–rain transition boundary [27 November 2013 (event A), 14–15 December 2013 (event C), 24 January 2015 (event F), 26 January 2015 (event G), and 22 February 2015 (event H)].

Although the number of events was rather limited, the storm events studied lasted multiple days and covered large areas, yielding totals of $\sim 11\,000$, $\sim 15\,000$, and ~ 2300 of rain, snow, and mixed-phase ASOS

observations, respectively, and ~ 3200 , ~ 2100 , and ~ 970 mPING hourly observations.

4. Results

a. Model performance skill in determining surface precipitation phase

In this section we examine the HRRR model's performance skill in predicting the surface precipitation phase. This was done by applying the evaluation matrix described in Ikeda et al. (2013, their Table 2). The results from the cases examined in this study are compiled in Table 2. The matrix is built by comparing predictions to ASOS observations within close spatial proximity following a simple procedure. First, model predictions from a $24\text{ km} \times 24\text{ km}$ neighborhood box area centered at a grid point closest to each ASOS observational site are collected (Fig. 1c). Then, for each observation–model pair at each evaluation time, the fraction of area forecasted as snow, rain, and mixed-phase precipitation, as well as no precipitation, is computed and assigned to the matrix cells of a corresponding ASOS-observed precipitation phase (Ikeda et al. 2013,

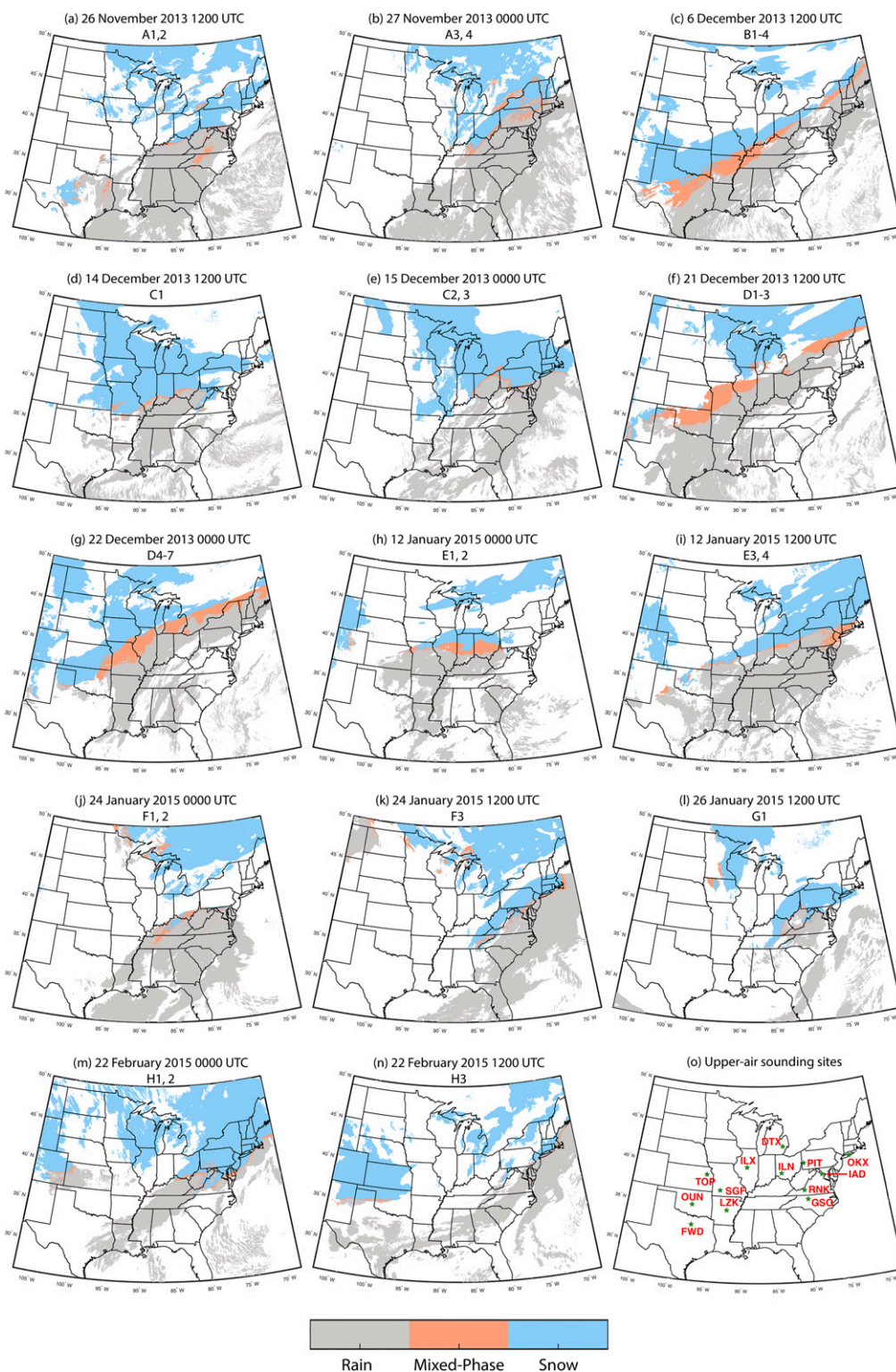


FIG. 2. (a)–(n) Precipitation phase maps from HRRR's 8-h forecasts for cases evaluated in this study. Each panel shows the event name, date, and time as seen in Table 1. (o) The upper-air sounding sites listed in Table 1.

TABLE 2. Evaluation matrix (percent) for the 8-h forecasts from each event examined in this study based on ASOS observations. The largest value in a row is highlighted in boldface. An ideal performance would mean having the highest values along the diagonal line (italicized in the first matrix).

		HRRR forecast					
Event		Snow	Mixed phase	Rain	NP	No. of observation	
A	26–28 Nov 2013						
	ASOS	Snow	75	3	2	20	1124
		Mixed phase	15	17	66	2	209
		Rain	<1	2	96	2	3123
		NP	5	<1	9	86	14 541
	UP	23	2	50	25	1637	
B	5–7 Dec 2013						
	ASOS	Snow	86	6	1	7	742
		Mixed phase	23	55	11	11	562
		Rain	<1	7	85	8	1441
		NP	7	1	24	68	12 076
	UP	22	7	40	31	1926	
C	13–15 Dec 2013						
	ASOS	Snow	92	3	1	4	2670
		Mixed phase	30	34	32	4	226
		Rain	2	4	89	5	1433
		NP	7	<1	13	79	13 376
	UP	43	3	24	30	1967	
D	20–24 Dec 2013						
	ASOS	Snow	87	1	1	11	1554
		Mixed phase	14	58	22	6	541
		Rain	<1	4	92	4	3404
		NP	5	1	20	74	18 807
	UP	30	5	31	34	3947	
E	11–12 Jan 2015						
	ASOS	Snow	92	1	2	5	1131
		Mixed phase	14	37	45	4	320
		Rain	1	5	90	4	2132
		NP	3	1	19	77	20 468
	UP	28	5	45	22	1942	
F	23–24 Jan 2015						
	ASOS	Snow	86	5	6	3	739
		Mixed phase	41	18	37	4	136
		Rain	3	3	91	3	2034
		NP	4	1	9	86	21 011
	UP	16	3	44	37	2005	
G	26 Jan 2015						
	ASOS	Snow	94	2	2	2	1056
		Mixed phase	41	10	33	16	7
		Rain	4	4	86	6	223
		NP	4	<1	5	90	9349
	UP	41	2	17	40	757	
H	21–22 Feb 2015						
	ASOS	Snow	92	3	2	3	1835
		Mixed phase	37	25	34	4	272
		Rain	5	6	85	4	902
		NP	11	<1	14	75	11 555
	UP	44	3	19	34	1699	

their Table 2). Finally, the sum of the fractions in each matrix cell (over the duration of a precipitation event of interest) is computed and normalized by the total of fractions added across a particular row (i.e., the ASOS-observed precipitation phase). The best model

performance would be seen by the highest numerical values falling along a diagonal line in Table 2.

Consistent with Ikeda et al. (2013), the forecast skill for areas of snow and rain are high, having the largest fractional values in the same precipitation-phase category as

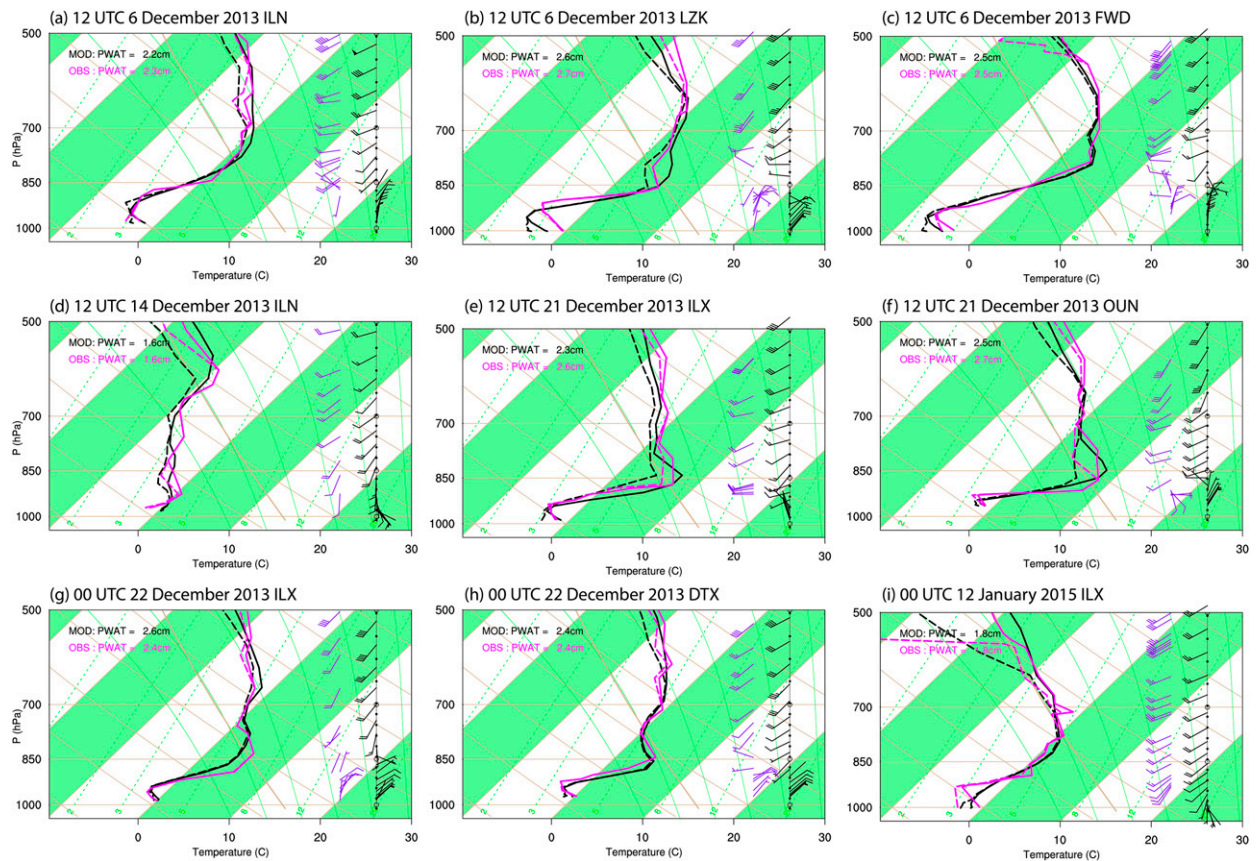


FIG. 3. Skew- T diagrams when both the 8-h model forecast and surface observation at a nearby or collocated ASOS site reported mixed-phase precipitation at locations and times indicated. Refer to Table 1 and Fig. 2 for radiosonde station names and locations. Temperatures (solid line) and dewpoint temperatures (dashed line) from the observations are shown in magenta. Those from the HRRR model are in black. Wind barbs from the observations (purple) and model (black) are also shown. Precipitable water (PWAT) from the model (MOD) and observations (OBS) are indicated in the top-left corner of each panel.

observed, but the model is generally less skillful in the mixed-phase precipitation areas than the rain and snow areas. The tendency for lower skill in the mixed-phase precipitation area is commonly found in schemes that determine precipitation types (e.g., Reeves et al. 2014; Reeves et al. 2016). It is important to note that although it cannot be directly inferred from the evaluation matrix alone, the spatial extent and general locations of mixed-phase precipitation predicted by the HRRR forecasts agreed qualitatively well with the ASOS and mPING observations, as found in the previous study (Ikeda et al. 2013). This is also a general indication of relatively skillful surface temperature forecasts and predicted microphysical properties.

Table 2 also indicates that the HRRR model performed well in predicting ASOS-observed mixed-phase precipitation during events B and D (5–7 and 20–24 December 2013, respectively), having the largest skill value associated with the correct precipitation phase. These two cases share common characteristics; they are

from a large-scale synoptic system moving across the Midwest and toward the East Coast that generated a swath of well-defined freezing rain area across the eastern United States (Figs. 2c,f,g). For other cases, the evaluation matrix reveals that the HRRR model tended to forecast ASOS-observed mixed-phase precipitation as rain more often than snow when a prediction error occurred. Cold-air damming cases (events A and E; Fig. 2a,i) are among such cases. The exceptions are events G (26 January 2015) and H (21–22 February 2015) when the model predicted snow more often than rain when the ASOS observations reported mixed-phase precipitation. These two cases generated a narrow rain–snow transition boundary (Figs. 2l–n).

Below, we will examine the observed and model-predicted surface temperatures and soundings for three groups of outcomes: 1) when a correct prediction of mixed-phase precipitation was made, 2) when rain was predicted but mixed-phase precipitation was observed or vice versa, and 3) when snow was predicted

TABLE 3. In addition to the event date and time, shown are the model-predicted and observed surface air temperatures T_s at the lowest observational or model height; the T_s bias, which is taken as the model minus the observations; the heights at the top and bottom boundaries of the elevated warm layer (where $T = 0^\circ\text{C}$) (H_{\max} and H_{\min} , respectively); and the thickness of the warm layer dH for the freezing rain soundings shown in Fig. 3. The lowest reported height and the model's lowest vertical level at the sounding site location are listed in the rightmost column.

Date and time	Location	T_s ($^\circ\text{C}$)		T_s bias	H_{\max} (m MSL)		H_{\min} (m MSL)		dH (m)		Lowest height (m MSL)	
		Model	Obs	M – O	Model	Obs	Model	Obs	Model	Obs	Model	Obs
1200 UTC 6 Dec 2013	ILN	−1.4	−2.2	0.8	2928	2609	1635	1461	1293	1148	314	382
	LZK	−2.0	−0.3	−1.7	3492	3168	1022	1136	2470	2032	156	173
	FWD	−4.5	−3.5	−1.0	3272	3352	1460	1404	1812	1948	191	220
1200 UTC 21 Dec 2013	ILX	−1.0	−1.5	0.5	2596	2763	761	946	1835	1817	185	210
	OUN	−1.1	−1.1	0	2765	2673	619	714	2146	1959	364	395
0000 UTC 22 Dec 2013	ILX	0.1	0.0	0.1	2622	2442	810	741	1812	1701	185	173
	DTX	−0.2	0.2	−0.4	2276	2165	806	964	1470	1201	316	329
0000 UTC 12 Jan 2015	ILX	−1.3	−0.5	−0.8	2279	2356	1194	1043	1085	1313	185	208

but mixed-phase precipitation was observed (refer to Table 1).

b. Evaluation using temperature profiles and surface temperatures

Figure 3 shows a comparison of observed and model-based skew- T diagrams when the HRRR model correctly predicted mixed-phase precipitation at the surface when compared with the nearest or collocated ASOS observation. With the exception of Fig. 3d (event C; corresponding to Fig. 2d), the cases are observed freezing rain events. All of these freezing rain episodes occurred either over a widespread area across the Midwest or the East Coast over a prolonged time (events B, D, and E; Figs. 2c,g,h). All model-predicted and observed profiles present a classical freezing rain temperature profile (e.g., Stewart 1985; Zerr 1997; Stewart et al. 2015) characterized by 1) a subfreezing surface layer, 2) an elevated inversion layer with a maximum temperature $> 0^\circ\text{C}$ (i.e., elevated warm layer), and 3) an adjacent layer aloft where the temperature rapidly cools to $< 0^\circ\text{C}$ with increasing height and that is at or nearly saturated with respect to ice. The thickness of the observed elevated warm layer ranges from ~ 1100 to 2000 m (Table 3), which is a typical thickness seen in classical freezing rain profiles (Zerr 1997). The model profiles' depth of the elevated warm layer is within ~ 440 m of the observed depth and matches very well (Table 3). The differences in the 0°C height at the top H_{\max} and bottom H_{\min} of the elevated warm layer are between -170 and 320 m and between ~ -190 and 170 m, respectively (Table 3). The vertical resolution of the HRRR model is as small as ~ 20 m near the surface and increases up to ~ 500 m near the 700-hPa level, which is the pressure level close to H_{\max} in most of the soundings shown (Fig. 3). The radiosonde data have a similar vertical

resolution. Considering the vertical model levels, the agreement of the 0°C height associated with H_{\max} and H_{\min} between the observation and model is quite impressive. The near-surface air temperature, taken from the model level closest to the surface, is also close to the observations, having a bias of $< 2^\circ\text{C}$ (Table 3).

Figure 4 shows examples of the time evolution of the ASOS-observed and model-predicted precipitation phase, observed temperature and dewpoint temperature (from ASOS), model-predicted temperature, and 1-h total precipitation comparison from the 5–7 December 2013 and 11–12 January 2015 events (events B and E; Table 2) for three ASOS and corresponding sounding sites where the model correctly predicted the surface precipitation phase at the radiosonde observation time. There is a cold bias at Dallas, Texas (DFW; see the appendix for a listing of ASOS station locations), but the overall temperature trend agrees with the observations, which is partly the result of a general agreement in the precipitation trend. The temperature stays steady near 0°C in the HRRR results and observations at the other two locations: Cincinnati, Ohio (CVG), and Coles County, Illinois (MTO). When freezing rain was reported, the model correctly predicted the predominant precipitation phase as mixed-phase precipitation in the neighborhood box area at the ASOS sites shown in the figure. Overall, the model-predicted freezing rain was persistent and the areal coverage also agreed well with the observations in these cases and, thus, produced the highest values in the mixed-phase category in the evaluation matrix for the 5–7 and 20–24 December 2013 events (events B and D; Table 2).

Figure 3d is from a precipitation event where a narrow rain-to-snow transition boundary moved across the Wilmington, Ohio (ILN), radiosonde site (event C; Fig. 2d). Both the observed and model-predicted

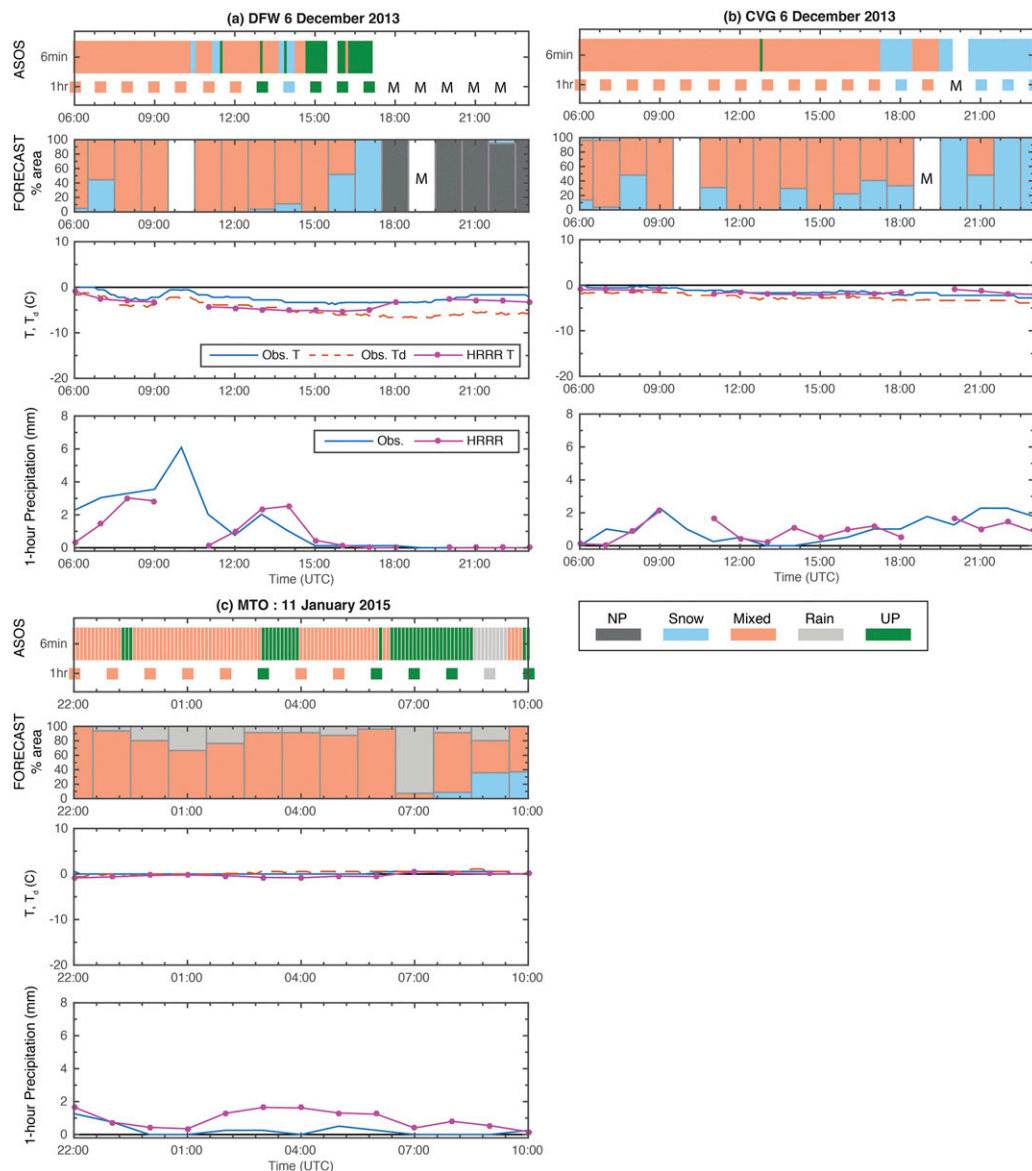


FIG. 4. ASOS and HRRR model precipitation phase at (a) DFW near FWD and (b) CVG near ILN on 6 Dec 2013 (event B) and (c) MTO near ILX on 11 Jan 2015 (event E). For (a)–(c), the color-coded vertical lines in the top panels show the observed precipitation phase in increments of 6 min (white space indicates missing data), while colored squares represent the observations on the hour with the ± 6 -min temporal window taken into account (M is for missing data). The second panels show the percent of the neighborhood area covered with model-predicted snow (light blue), rain (light gray), and mixed-phase precipitation (pink) based on the 8-h forecasts at the ASOS site; dark gray indicates no precipitation. The third panels show ASOS surface temperature T , dewpoint temperature T_d , and model-predicted surface temperature from 8-h forecasts. The bottom panels show the 1-h precipitation amounts (mm).

profiles are representative of the wet snow temperature profile shown in [Stewart et al. \(2015, their Fig. 2b\)](#). The aviation routine weather reports (METARs) from ILN alternately reported snow and rain, and the surface temperature varied between -1° and 1°C from ~ 1100 to 1600 UTC 14 December 2013. The METAR observations are clearly reflected in the ILN skew- T sounding

([Fig. 3d](#)), which shows a weak elevated inversion layer close to the surface with a temperature and dewpoint temperature maximum just high enough to initiate melting. Although the details of the model profile do not perfectly trace the observed ILN skew- T sounding, the model profile nicely captures the overall vertical structure of the observed dry- and wet-bulb temperatures.

The model-predicted surface temperature stayed nearly constant at 0°C when mixed-phase precipitation was reported (not shown).

The skew- T soundings when the HRRR model indicated rain but ASOS observations reported mixed-phase precipitation or vice versa are shown in Fig. 5. Figures 5a–f are from a long period of freezing rain over a broad area or area of cold-air damming (events A, D, E, and F; Fig. 2a,f,h–k); while Figs. 5g–h are from a narrow rain–snow transition zone passing the sounding site over a short period of time (events G and H; Figs. 2l–n). Except for Figs. 5c,h, the model predicted rain when mixed-phase precipitation was observed at corresponding ASOS sites (Table 1). Most of the model temperature profiles closely follow the upper-air observations, as in Fig. 3. When a sharp, near-surface inversion layer is present in the observed soundings (i.e., an indication of freezing rain), the model also predicts a surface inversion layer in general. The precipitation phase forecast error is due to a surface temperature bias (mostly a warm bias in the cases examined), which may be partly related to some temporal lag in the precipitation phase transition. However, in many of the cases evaluated in this study, the forecast was very close to the observed results. As an example, Fig. 6a depicts a time evolution of precipitation phase and temperature at Washington Dulles International Airport, Sterling, Virginia (IAD), associated with the skew- T sounding comparison shown in Fig. 5g—one of the cases with a narrow rain–snow boundary (event G; 26 January 2015). According to the ASOS observations, the surface temperature started to decrease with an onset of precipitation at ~0900 UTC and rapidly dropped to ~0°C at ~1200 UTC after a peak in precipitation (i.e., due to evaporative cooling). Around this time, ASOS reported a rain–snow mixture, and the transition from rain to snow occurred over less than 1 h. A similar temporal evolution was seen from the model-predicted surface temperature, precipitation rate, and precipitation phase (i.e., a gradual increase in the fraction of mixed-phase precipitation between 1200 and 1800 UTC), but the evolution lagged the observations by several hours. As a result, the surface precipitation phase from the model was rain instead of freezing rain for the 1200 UTC sounding comparison. Note that both the model-predicted rain and snow mixing ratio in the lowest model level were nonzero at 1200 UTC, but the snow–rain ratio was lower (likely because of the above-freezing temperature environment) than the threshold implemented in the HRRR's precipitation-type algorithm and, thus, designated rain at this location.

A precipitation phase transition occurred twice at Brookhaven, New York (OKX), on 22 February 2015 (event H). The skew- T sounding shown in Fig. 5h is

associated with the second phase change. Although the precipitation phase forecast (mixed phase) did not agree with the observation (rain) at the time of the skew- T observations, the time history plot for a nearby site shows that the phase change timing was very well represented by the model based on the temporal trend of the precipitation phase distribution in the neighborhood box (Fig. 6b). The first phase change occurring at ~0500 UTC is also closely predicted by the model. The ASOS-observed and HRRR-predicted temperatures agree very well before 1400 UTC.

The prediction errors in the precipitation phase at Springfield, Missouri (SGF), at 1200 UTC 21 December 2013 (event D; Figs. 5b and 6c) and at ILN at 0000 UTC 12 January 2015 (event E; Figs. 5c and 6d) are due to a very small temperature bias at the surface: a warm bias of <1°C at SGF and a cold bias of <2.0°C at ILN. Additionally, both of the sites were near the edge of the predicted mixed-phase precipitation area at this time (as depicted by the precipitation phase evolution in Figs. 6c,d and 2c,h), implying that the forecast was almost correct. At these sites, the predicted and observed precipitation trends also agree well.

Freezing rain episodes from the 26 November 2013 (event A) and 12 January 2015 (event E) cases at Greensboro, North Carolina (GSO), and IAD, respectively (Figs. 5a,d), involved cold-air damming (e.g., Bell and Bosart 1988; Rackley and Knox 2016) east of the Appalachian Mountains, which led to a long-lasting widespread freezing rain episode (lasting >3 h at many surrounding ASOS sites). Figure 7a shows time history plots for GSO on 26 November 2013. The temperature bias at this location at ~1200 UTC is almost negligible, and the temperature trend is similar to the observations, except that the period of steady cold surface air (~0°C) is slightly shorter in the model forecast than the observations. Perhaps this is related to the precipitation rate difference between the forecast and the observations (Fig. 7a, bottom); the observed temperature decreased to 0°C, associated with an increase in precipitation intensity at ~1100 UTC, and stayed ~0°C until the precipitation rate started to decrease after 1800 UTC, while the corresponding increase and decrease of the precipitation rate in the model do not quite match in time. However, the forecast was not far off from the observations. Note that 8-h forecasts are shown here and, perhaps, a shorter forecast length may yield different results. During the period of steady cold surface air, the fraction of the predicted precipitation phase indicated mixed-phase precipitation within the neighborhood box area at this site (Fig. 7a, second panel). A 2D map of the model-predicted precipitation phase valid at 1200 UTC 26 November 2013 (time corresponding to Fig. 5a) shows a patch of mixed precipitation in western

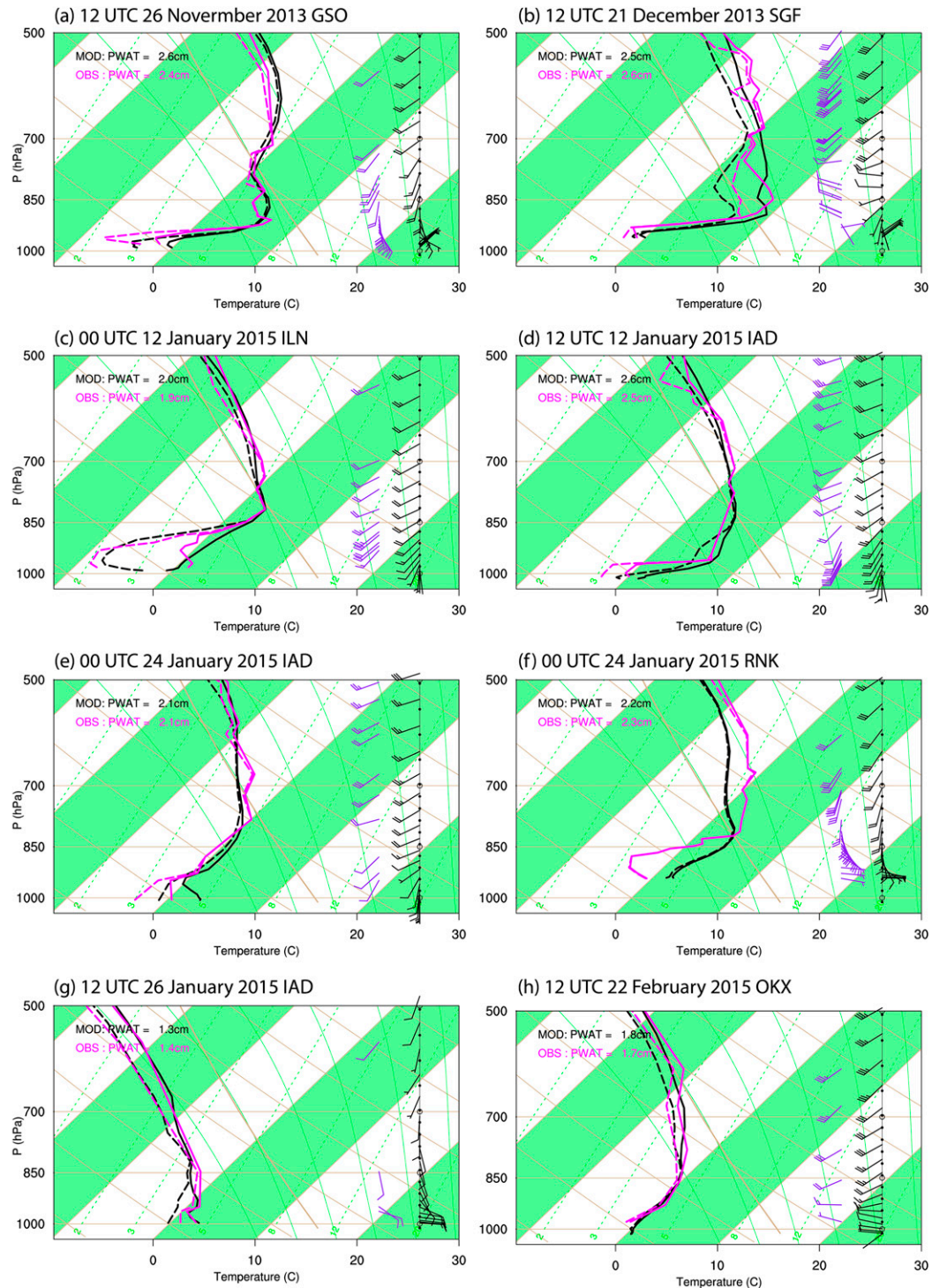


FIG. 5. As in Fig. 3, but for cases where the observations reported mixed-phase precipitation but the HRRR forecast indicated rain or vice versa.

Virginia and North Carolina (Fig. 7c), revealing that cold-air damming was indeed in the forecast. Inspection of hourly forecasts throughout the event suggests that a similar warm bias in this area led to spatial coverage that

was not always as widespread and the period of freezing rain not as steady as observed by ASOS and mPING.

A more significant warm bias in the areas of cold-air damming was found for the 12 January 2015 case (event E;

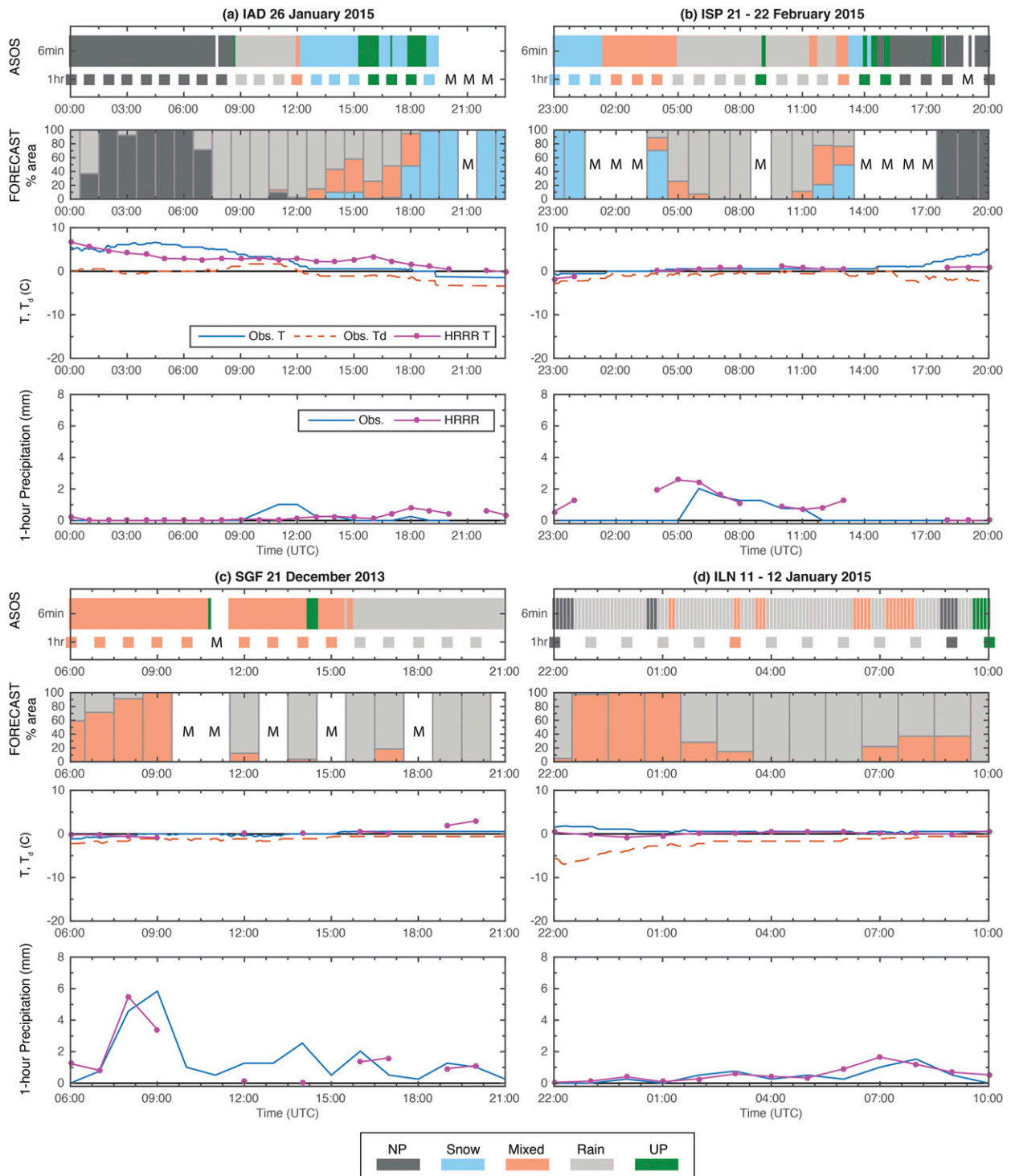


FIG. 6. As in Fig. 4, but for (a) IAD on 26 Jan 2015, (b) Islip, NY (ISP) near OKX on 21–22 Feb 2015, (c) SGF on 21 Dec 2013, and (d) ILN on 11–12 Jan 2015.

Figs. 5d, 7b, and 7d). A 2D map of the precipitation phase for this case (Fig. 7d) shows that the model-predicted area of mixed-phase precipitation does not extend southward enough into Virginia. A warm bias

as large as 4°C was found at locations where freezing rain was observed by ASOS and mPING. The precipitation rate at IAD after 1200 UTC is higher in the observations than the forecast, which may have led to

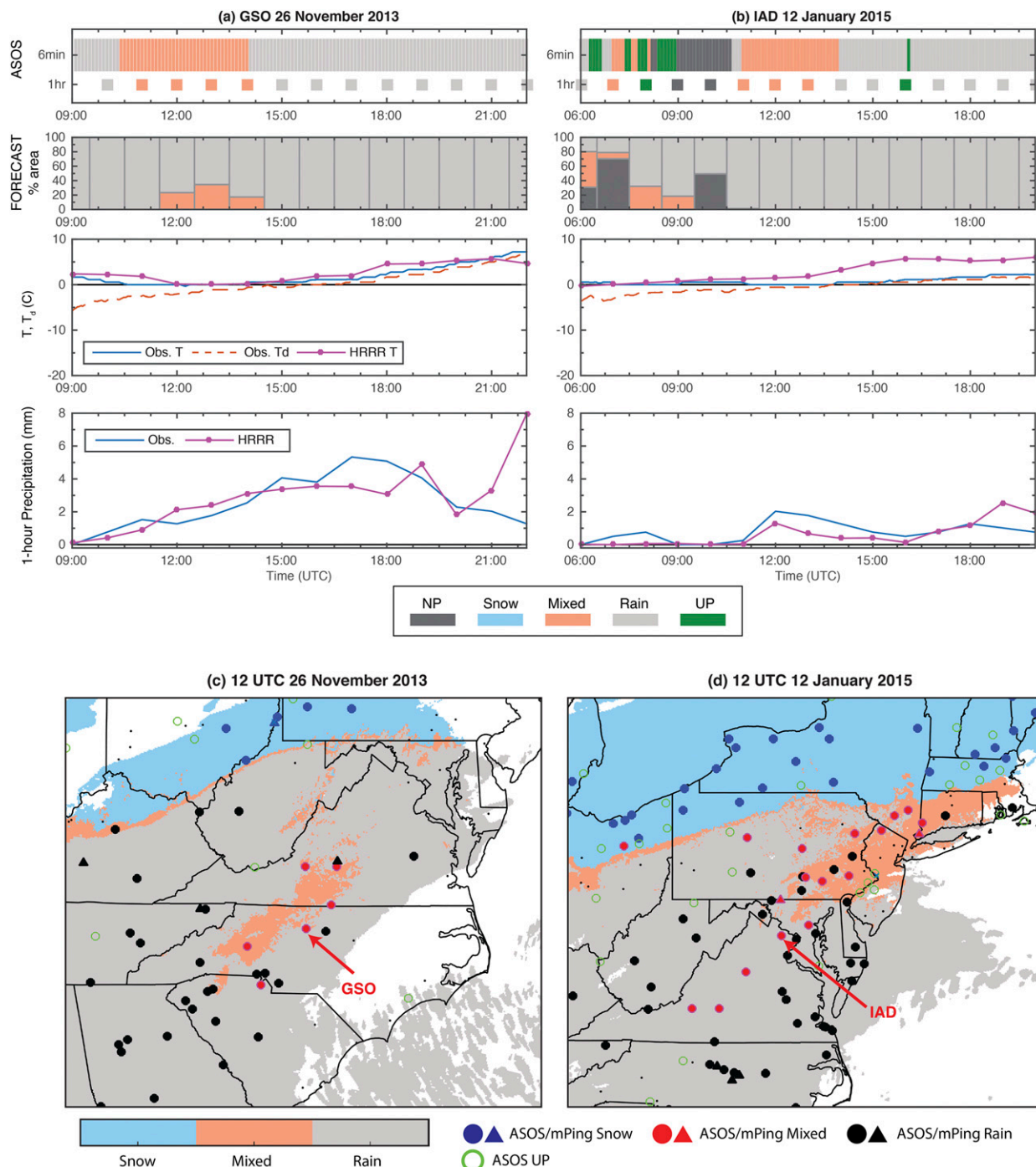


FIG. 7. As in Fig. 4, but for (a) GSO on 26 Nov 2013 and (b) IAD on 12 Jan 2015. (c),(d) Model-predicted precipitation phase (color-filled areas) overlaid with ASOS (circles) and mPING (triangles) observations valid at the indicated times. Figures 5a,d are skew- T sounding comparisons corresponding to (c) and (d), respectively. Locations of the GSO and IAD soundings and ASOS sites are indicated.

the longer period of time that the surface temperature stayed $\sim 0^{\circ}\text{C}$. For both of these cases the evaluation matrix (Table 2) shows the largest value in the rain category when mixed-phase precipitation was observed, which is attributed to the warm bias in cold-air

damming regions during these long and widespread freezing rain episodes.

Similarly, the incorrect precipitation phase prediction at the surface on 24 January 2015 (event F, Figs. 5e–f) was from a warm bias in the surface

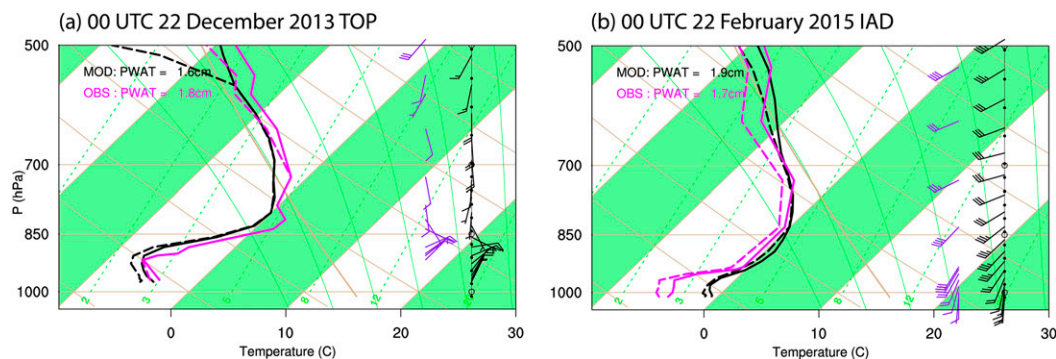


FIG. 8. As in Fig. 3, but for cases where the observations indicated mixed-phase precipitation but the HRRR forecast called for snow.

temperature. This freezing rain episode occurred while a strong low pressure system moved northward over the mid-Atlantic states and into the upper Northeast (Figs. 2j–k). The transition from rain to snow occurred over a short period at ~0000 UTC 24 January 2015 at IAD (Fig. 5e) associated with a weakly defined transition zone similar to the 26 January 2015 case at IAD (event G; Fig. 6a). The temperature profile clearly indicated a warm bias (3°C) at the surface. In this case, there was also a warm bias aloft in a near-isothermal layer (~880–730 hPa), where the model and observation both exhibit a temperature close to 0°C, just above the shallow near-surface inversion layer. Although the bias was only ~0.5°C in this layer, this likely contributed to altering the precipitation type reaching the surface.

The 24 January 2015 case (event F) also involved a pool of cold air (~0°C), in a confined area in western Virginia to the east of the Appalachian Mountains after a passage of the rain–snow transition boundary. However, because of a warm bias the forecast did not represent the cold-air damming well. This is reflected in the disagreement in the lower-altitude profile structure between the model and the Roanoke, Virginia (RNK), skew-*T* sounding (Fig. 5f). The surface inversion is much weaker and the upper layer above the inversion layer is colder in the model than in the observations, implying very different microphysical processes.

Figure 8 shows two skew-*T* soundings where the model predicted snow but mixed-phase precipitation was observed at the surface by ASOS. Characteristic features of the observed temperature profiles are well represented by the HRRR model in both cases, although the vertical temperature gradient of the elevated temperature inversion layer near the surface in the forecast profile is not as large as the observations at IAD at 0000 UTC 22 February 2015 (Fig. 8b).

Factors that contributed to the incorrect precipitation phase prediction at the surface at 0000 UTC 22 December 2013 (event D; Fig. 8a) were a cold bias in surface temperature (Fig. 9a, second panel), which may be related to a higher precipitation rate in the forecast before 0300 UTC, and a cold bias in the elevated warm layer (above ~850 hPa). The 2D map of the precipitation phase forecast at the time of the Topeka, Kansas (TOP), skew-*T* sounding reveals that TOP was close to the area of widespread freezing rain [Fig. 9c; surface observations are marked with red circles (ASOS) or triangles (mPING) where freezing rain was reported]. The maximum temperature observed in this elevated warm layer is 1.8°C. The elevated layer with ~0°C temperature is likely not deep enough to melt all snow particles completely but is deep enough to produce wet snowflakes and a rain–snow mixture. METARs at TOP indeed indicate light freezing rain between 2158 UTC 21 December 2013 and 0128 UTC the following day. However, the model's inversion layer does not go beyond the 0°C isotherm, causing differing microphysical species in the near-surface layer. Nonetheless, the forecast model very nicely predicts the vertical structure of such a critical phase-transitional region of the storm system.

Precipitation phase changed from snow to mixed-phase precipitation after 2300 UTC 21 February 2015 near Washington (event H; Figs. 8b, 9b, and 9d). Beginning ~2300 UTC, mPING data included a few reports of a rain–ice pellet mixture and freezing rain among the dominant snow–ice pellet reports in the area between IAD and Washington's Ronald Reagan International Airport (DCA). Soon after 0010 UTC, freezing rain observations in the mPING reports became more dominant than the snow–ice pellet reports. At IAD, freezing rain and a snow–ice pellet mixture was reported until 0015 UTC, then ice pellets together with freezing rain were reported until 0306 UTC, and

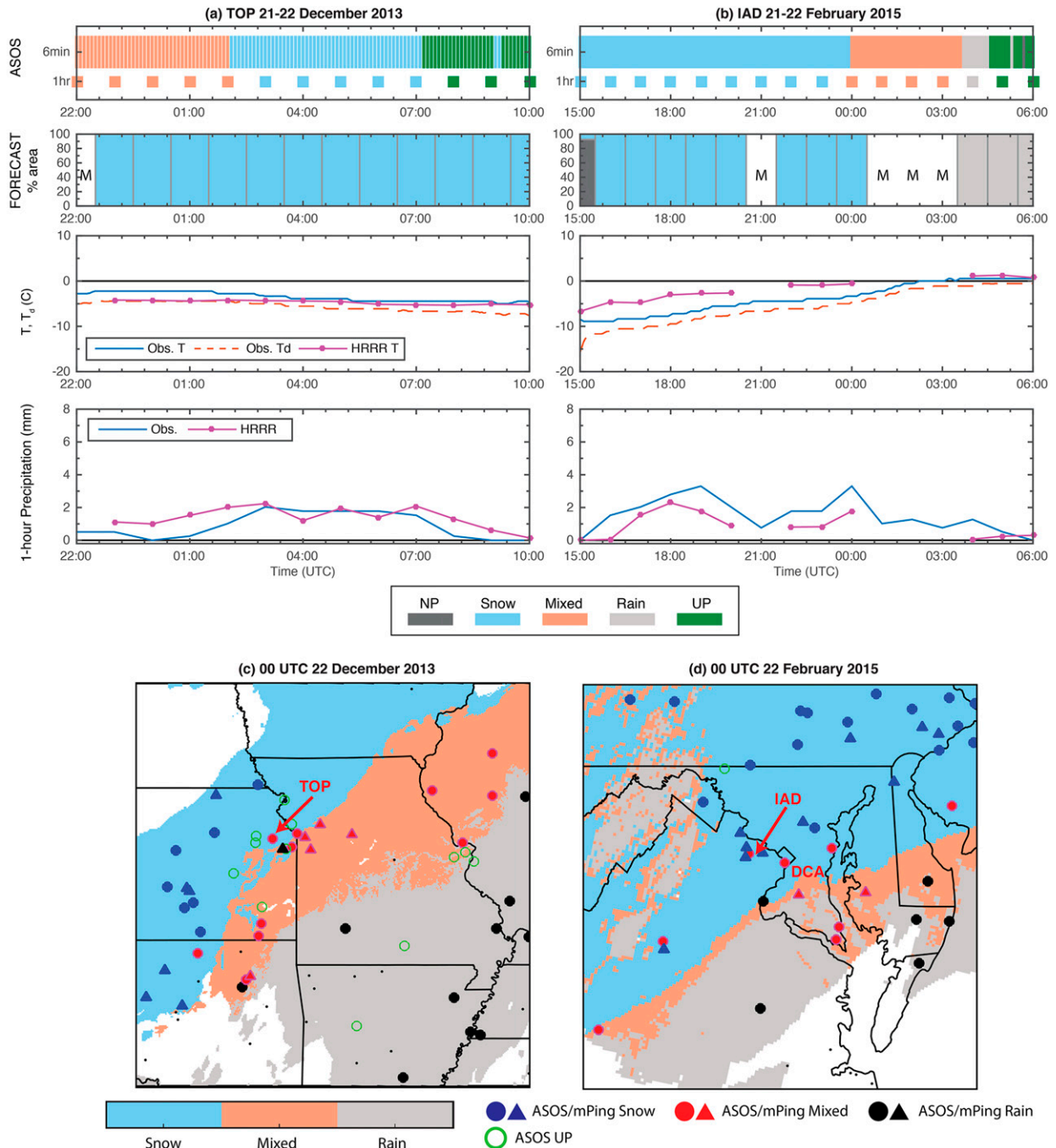


FIG. 9. As in Fig. 4, but at (a) TOP on 22 Dec 2013 and (b) IAD on 22 Feb 2015. (c), (d) As in Figs. 7c,d, but corresponding to the skew- T sounding comparisons shown in Figs. 8a,b.

then simply freezing rain until 0344 UTC followed by rain. Although Fig. 9d shows IAD's mixed-phase observations surrounded by mPING reports of snow at 0000 UTC 22 February 2015, all mPING reports from this region changed to mixed phase by 0100 UTC. A well-defined cold layer (refreezing layer) below the elevated inversion layer in the observed skew- T sounding

(Fig. 8b) corresponds well with these precipitation-type reports. The model clearly shows snow in this region, and the rain-snow transition zone is well south of IAD at 0000 UTC. Unfortunately, the model data are missing between 0100 and 0300 UTC, preventing us from verifying the location of the phase change boundary during this time period (which likely took

place according to the temperature trend seen in Fig. 9b). However, examination of a 2D map of predicted precipitation phase and observations for later times indicates that the model's phase transition zone lagged behind the phase transition zone observed by ASOS and mPING as the storm system propagated northward along the Eastern Seaboard. The high value in the evaluation matrix (Table 2) associated with snow forecasts when mixed-phase precipitation was reported by ASOS is clearly the result of such a temporal lag. Based on all of the cases evaluated, such an obvious/significant temporal lag in the phase transition was not systematically found in other cases.

5. Summary and concluding remarks

A numerical weather prediction model's ability to capture properly precipitation-phase transitions at the surface is clearly associated with its skill in correctly representing the thermodynamic profile aloft and microphysical processes (e.g., melting, refreezing). The present study expanded upon the earlier work of Ikeda et al. (2013), which revealed relatively lower performance skill of the HRRR model for mixed-phase precipitation compared with snow and rain. In this study, routine upper-air sounding observations along with ASOS and mPING surface data in mixed-phase precipitation regions were used to compare the model profiles against to investigate possible reasons for precipitation-phase forecast errors for 14 cases from the 2013/14 and 2014/15 winter seasons.

When both the observational and model data indicated mixed-phase precipitation at the surface, the HRRR model represented the observed temperature profile well. In particular, characteristic features of a freezing rain profile, including the depth, height, and maximum temperature of an elevated inversion layer, as well as the depth of a subfreezing surface layer, agreed well with the observations.

Cases when the HRRR model predicted rain but the observations indicated mixed-phase precipitation were generally associated with a warm surface temperature bias. Yet the vertical structure of the temperature profile from the model was still representative of the observed soundings. The surface temperature for these cases was near 0°C, and the bias was usually less than 2°C. The time evolution of predicted and ASOS-observed precipitation phase and temperature showed close agreement in temperature trend and phase change (although a temporal lag was present in some cases), demonstrating that the model mostly agreed with the observations.

The surface temperatures from the HRRR model forecasts were too warm yielding precipitation phase

errors in the examined cases with thin cold-air layers related to cold-air damming, which produced long-lasting and widespread freezing rain in the eastern United States. For a few of the examined cases, the predicted precipitation phase maps showed a region of mixed-phase precipitation associated with the cold-air damming and observed mixed-phase region; however, the spatial extent was smaller and the temporal duration was shorter than the observations. For these cases, the evaluation matrix indicated a strong trend in misclassifying the observed mixed-phase precipitation as rain, and while the model temperature and dewpoint profiles closely followed the observations aloft, the surface subfreezing layer was missing or had a significant warm bias. The warm bias in surface temperature was as large as 4°C and was much larger than the "close call" cases mentioned above. This is perhaps partly related to the HRRR model not having enough evaporative cooling from precipitation (in terms of strength and duration) based on the time history comparison of the observed and predicted precipitation rates among other possible reasons that were not fully investigated in this study.

Among the 14 cases, only two skew-*T* soundings corresponded to occasions when the ASOS observation indicated mixed-phase precipitation but the model forecast was snow. Model profiles from these cases showed a very good level of agreement with the observations except at vertical levels having temperatures close to the 0°C isotherm, just above the near-surface inversion layer. In particular, because of the cold temperature bias at those levels, the particles did not go through a melting process and resulted in a mismatch in the surface precipitation phase.

The results presented in this study certainly do not cover all of the possible reasons for misclassifications of mixed-phase precipitation, which likely involves further model sensitivity tests to explore. The precipitation phase predicted by the HRRR may also be sensitive to the representativeness of mesoscale features and/or model initialization. The cases examined are limited by the availability of routine upper-air sounding data coinciding with mixed-phase precipitation events; therefore, a robust statistical evaluation could not be performed. Moreover, the prediction skill difference between ice pellets and freezing rain or ice pellets and snow, which impacts ground icing, was not addressed, because ASOS does not explicitly identify ice pellets (except at sites with human observers). Additionally, the cases examined in this study were only from the eastern United States, and the model performance for other parts of the United States where mixed-phase precipitation occurs is possibly different. For example, the northern Cascade region is frequently

impacted by freezing drizzle/rain and ice pellets (Bernstein 2000). Nevertheless, the current results reveal that the HRRR model is able to represent the overall vertical thermodynamic structure in the mixed-phase precipitation regions involving areas of a rain–snow transition and freezing rain, and that a proper forecast of the surface/near-surface temperature is critical for accurately depicting the precipitation phase.

Acknowledgments. This research was carried out in response to requirements of and funding from the Federal Aviation Administration (FAA) and the National Oceanographic and Atmospheric Administration (NOAA). Additional support was provided by the National Science Foundation (NSF). The views expressed are those of the authors and do not necessarily represent the official policy or position of the funding agencies. The thoughtful comments received from the reviewers were much appreciated.

APPENDIX

Upper-Air Sounding Site IDs and Locations That Appear in This Study

DTX	Detroit, Michigan
FWD	Fort Worth, Texas
GSO	Greensboro, North Carolina
IAD	Sterling, Virginia
ILN	Wilmington, Ohio
ILX	Lincoln, Illinois
LZK	Little Rock, Arkansas
OKX	Brookhaven, New York
OUN	Norman, Oklahoma
PIT	Pittsburgh, Pennsylvania
RNK	Roanoke, Virginia
SGF	Springfield, Missouri
TOP	Topeka, Kansas

REFERENCES

- Bell, G. D., and L. F. Bosart, 1988: Appalachian cold-air damming. *Mon. Wea. Rev.*, **116**, 137–161, doi:[10.1175/1520-0493\(1988\)116<0137:ACAD>2.0.CO;2](https://doi.org/10.1175/1520-0493(1988)116<0137:ACAD>2.0.CO;2).
- Benjamin, S. G., and Coauthors, 2016a: A North American hourly assimilation and model forecast cycle: The Rapid Refresh. *Mon. Wea. Rev.*, **144**, 1669–1694, doi:[10.1175/MWR-D-15-0242.1](https://doi.org/10.1175/MWR-D-15-0242.1).
- , J. M. Brown, and T. G. Smirnova, 2016b: Explicit precipitation-type diagnosis from a model using a mixed-phase bulk cloud-precipitation microphysics parameterizations. *Wea. Forecasting*, **31**, 609–619, doi:[10.1175/WAF-D-15-0136.1](https://doi.org/10.1175/WAF-D-15-0136.1).
- Bernstein, B. C., 2000: Regional and local influences on freezing drizzle, freezing rain, and ice pellet events. *Wea. Forecasting*, **15**, 485–508, doi:[10.1175/1520-0434\(2000\)015<0485:RALIOF>2.0.CO;2](https://doi.org/10.1175/1520-0434(2000)015<0485:RALIOF>2.0.CO;2).
- Burg, T., K. L. Elmore, and H. M. Grams, 2017: Assessing the skill of updated precipitation type diagnostics for the Rapid Refresh with mPING. *Wea. Forecasting*, **32**, 725–732, doi:[10.1175/WAF-D-16-0132.1](https://doi.org/10.1175/WAF-D-16-0132.1).
- Call, D. A., 2005: Rethinking snowstorms as snow events: A regional case study from upstate New York. *Bull. Amer. Meteor. Soc.*, **86**, 1783–1793, doi:[10.1175/BAMS-86-12-1783](https://doi.org/10.1175/BAMS-86-12-1783).
- , 2010: Changes in ice storm impacts over time: 1886–2000. *Wea. Climate Soc.*, **2**, 23–35, doi:[10.1175/2009WCAS1013.1](https://doi.org/10.1175/2009WCAS1013.1).
- Changnon, S. A., 2003: Characteristics of ice storms in the United States. *J. Appl. Meteor.*, **42**, 630–639, doi:[10.1175/1520-0450\(2003\)042<0630:COISIT>2.0.CO;2](https://doi.org/10.1175/1520-0450(2003)042<0630:COISIT>2.0.CO;2).
- Elmore, K. L., Z. L. Flamig, V. Lakshmanan, B. T. Kaney, V. Farmer, H. D. Reeves, and L. S. Rothfusz, 2014: mPING: Crowd-sourcing weather reports for research. *Bull. Amer. Meteor. Soc.*, **95**, 1335–1342, doi:[10.1175/BAMS-D-13-00014.1](https://doi.org/10.1175/BAMS-D-13-00014.1).
- , H. M. Grams, D. Apps, and H. D. Reeves, 2015: Verifying forecast precipitation type with mPING. *Wea. Forecasting*, **30**, 656–667, doi:[10.1175/WAF-D-14-00068.1](https://doi.org/10.1175/WAF-D-14-00068.1).
- Goodwin, L. C., 2003: Weather-related crashes on U.S. highways in 2001. Mitretek Systems, Inc., Rep. prepared for U.S. Dept. of Transportation, 5 pp. [Available online at <https://ops.fhwa.dot.gov/weather/docs/2001CrashAnalysisPaperV2.doc>.]
- Grout, T., Y. Hong, J. Basara, B. Balasundaram, Z. Kong, and S. T. S. Bukkapatnam, 2012: Significant winter weather events and associated socioeconomic impacts (federal aid expenditures) across Oklahoma: 2000–10. *Wea. Climate Soc.*, **4**, 48–58, doi:[10.1175/WCAS-D-11-00057.1](https://doi.org/10.1175/WCAS-D-11-00057.1).
- Ikeda, K., M. Steiner, J. Pinto, and C. Alexander, 2013: Evaluation of cold-season precipitation forecasts generated by the hourly updating High-Resolution Rapid Refresh model. *Wea. Forecasting*, **28**, 921–939, doi:[10.1175/WAF-D-12-00085.1](https://doi.org/10.1175/WAF-D-12-00085.1).
- Lackmann, G. M., K. Keeter, L. G. Lee, and M. B. Ek, 2002: Model representation of freezing and melting precipitation: Implications for winter weather forecasting. *Wea. Forecasting*, **17**, 1016–1033, doi:[10.1175/1520-0434\(2003\)017<1016:MROFAM>2.0.CO;2](https://doi.org/10.1175/1520-0434(2003)017<1016:MROFAM>2.0.CO;2).
- National Weather Service, 1998: Automated Surface Observing System (ASOS) user's guide. NOAA/NWS, 61 pp. [Available online at <http://www.nws.noaa.gov/asos/pdfs/aum-toc.pdf>.]
- Rackley, J. A., and J. A. Knox, 2016: A climatology of southern Appalachian cold-air damming. *Wea. Forecasting*, **31**, 419–432, doi:[10.1175/WAF-D-15-0049.1](https://doi.org/10.1175/WAF-D-15-0049.1).
- Ramsay, A. C., 1997: Freezing rain-detection and reporting by the Automated Surface Observing System (ASOS). Preprints, *First Symp. on Integrated Observing Systems*, Long Beach, CA, Amer. Meteor. Soc., J65–J69.
- Rauber, R. M., L. S. Olthoff, M. K. Ramamurthy, and K. E. Kunkel, 2001: Further investigation of a physically based, non-dimensional parameter for discriminating between locations of freezing rain and ice pellets. *Wea. Forecasting*, **16**, 185–191, doi:[10.1175/1520-0434\(2001\)016<0185:FIOAPB>2.0.CO;2](https://doi.org/10.1175/1520-0434(2001)016<0185:FIOAPB>2.0.CO;2).
- Reeves, H. D., 2016: The uncertainty of precipitation-type observations and its effect on the validation of forecast precipitation type. *Wea. Forecasting*, **31**, 1961–1971, doi:[10.1175/WAF-D-16-0068.1](https://doi.org/10.1175/WAF-D-16-0068.1).
- , K. L. Elmore, A. Ryzhkov, and T. Schuur, 2014: Sources of uncertainty in precipitation-type forecasting. *Wea. Forecasting*, **29**, 936–953, doi:[10.1175/WAF-D-14-00007.1](https://doi.org/10.1175/WAF-D-14-00007.1).
- , A. V. Ryzhkov, and J. Krause, 2016: Discrimination between winter precipitation types based on spectral-bin microphysical modeling. *J. Appl. Meteor. Climatol.*, **55**, 1747–1761, doi:[10.1175/JAMC-D-16-0044.1](https://doi.org/10.1175/JAMC-D-16-0044.1).

- Sankaré, H., and J. M. Thériault, 2016: On the relationship between the snowflake type aloft and the surface precipitation types at temperatures near 0°C. *Atmos. Res.*, **180**, 287–296, doi:[10.1016/j.atmosres.2016.06.003](https://doi.org/10.1016/j.atmosres.2016.06.003).
- Sims, E. M., and G. Liu, 2015: A parameterization of the probability of snow–rain transition. *J. Hydrometeor.*, **16**, 1466–1477, doi:[10.1175/JHM-D-14-0211.1](https://doi.org/10.1175/JHM-D-14-0211.1).
- Skamarock, W. C., and Coauthors, 2008: A description of the Advanced Research WRF version 3. NCAR Tech. Note NCAR/TN-475+STR, 113 pp., doi:[10.5065/D68S4MVH](https://doi.org/10.5065/D68S4MVH).
- Stewart, R. E., 1985: Precipitation types in winter storms. *Pure Appl. Geophys.*, **123**, 597–609, doi:[10.1007/BF00877456](https://doi.org/10.1007/BF00877456).
- , 1992: Precipitation types in the transition region of winter storms. *Bull. Amer. Meteor. Soc.*, **73**, 287–296, doi:[10.1175/1520-0477\(1992\)073<0287:PTITTR>2.0.CO;2](https://doi.org/10.1175/1520-0477(1992)073<0287:PTITTR>2.0.CO;2).
- , J. M. Thériault, and W. Henson, 2015: On the characteristics of and processes producing winter precipitation types near 0°C. *Bull. Amer. Meteor. Soc.*, **96**, 623–239, doi:[10.1175/BAMS-D-14-00032.1](https://doi.org/10.1175/BAMS-D-14-00032.1).
- Thériault, J. M., R. E. Stewart, and W. Henson, 2010: On the dependence of winter precipitation types on temperature, precipitation rate, and associated features. *J. Appl. Meteor. Climatol.*, **49**, 1429–1442, doi:[10.1175/2010JAMC2321.1](https://doi.org/10.1175/2010JAMC2321.1).
- Thompson, G., and T. Eidhammer, 2014: A study of aerosol impacts on clouds and precipitation development in a large winter cyclone. *J. Atmos. Sci.*, **71**, 3636–3658, doi:[10.1175/JAS-D-13-0305.1](https://doi.org/10.1175/JAS-D-13-0305.1).
- , P. R. Field, R. M. Rasmussen, and W. D. Hall, 2008: Explicit forecasts of winter precipitation using an improved bulk microphysics scheme. Part II: Implementation of a new snow parameterization. *Mon. Wea. Rev.*, **136**, 5095–5115, doi:[10.1175/2008MWR2387.1](https://doi.org/10.1175/2008MWR2387.1).
- Wade, C. G., 2003: A multisensory approach to detecting drizzle on ASOS. *J. Atmos. Oceanic Technol.*, **20**, 820–832, doi:[10.1175/1520-0426\(2003\)020<0820:AMATDD>2.0.CO;2](https://doi.org/10.1175/1520-0426(2003)020<0820:AMATDD>2.0.CO;2).
- Zerr, R. J., 1997: Freezing rain: An observational and theoretical study. *J. Appl. Meteor.*, **36**, 1647–1661, doi:[10.1175/1520-0450\(1997\)036<1647:FRAOAT>2.0.CO;2](https://doi.org/10.1175/1520-0450(1997)036<1647:FRAOAT>2.0.CO;2).